Coherent sub-femtosecond soft x-ray free-electron laser pulses with nonlinear compression

Eduard Prat ✉ ⓘ ; Alexander Malyzhenkov; Christopher Arrell ⓘ ; Paolo Craievich ⓘ ; Sven Reiche ⓘ ;
Thomas Schietinger ⓘ ; Guanglei Wang ⓘ

Check for updates

CrossMark

View
Online

Export
Citation

Coherent sub-femtosecond soft x-ray free-electron laser pulses with nonlinear compression

View Online   Export Citation   CrossMark

Eduard Prat,[1,a] Alexander Malyzhenkov,[2] Christopher Arrell,[1] Paolo Craievich,[1] Sven Reiche,[1] Thomas Schietinger,[1] and Guanglei Wang[1]

AFFILIATIONS

[1] Paul Scherrer Institut, CH-5232 Villigen PSI, Switzerland
[2] CERN, CH-1211 Geneva 23, Switzerland

[a]Author to whom correspondence should be addressed: eduard.prat@psi.ch

ABSTRACT

We demonstrate the generation of coherent soft x-ray free-electron laser (FEL) pulses with a duration below 1 fs using nonlinear compression with a low-charge electron beam (10 pC). The approach is simple, and it does not require any special hardware, so it can be readily implemented at any x-ray FEL facility. We present temporal and spectral diagnostics confirming the production of single-spike sub-femtosecond pulses for photon energies of 642 and 1111 eV. Our work will be important for ultrafast FEL applications requiring soft x-rays.

X-ray free-electron lasers (FELs) are unique scientific instruments to study matter at atomic time and length scales.[1–3] The FEL radiation is produced by a high-brightness electron beam traveling through an undulator beamline. Standard x-ray FEL facilities generate transversely coherent radiation with gigawatt powers and a duration of a few tens of femtoseconds.[4–10] Most of the FEL facilities are based on the self-amplified spontaneous emission (SASE) process,[11] which results in FEL pulses with multiple spikes in both time and spectral domains, thus with limited longitudinal coherence. There are different ways to improve the longitudinal coherence of FEL pulses, most importantly via seeding schemes.[7,12–14]

Short x-ray FEL pulses at the femtosecond level and below are required to study ultrafast atomic and molecular processes.[15] In particular, there is a strong scientific interest in sub-femtosecond FEL pulses in the soft x-ray regime to study coherent electron motion.[16] Another advantage of shortening the pulse duration is related to the longitudinal coherence: if the pulses are made of only one spike, they are also fully coherent. The lower limit of the FEL pulse duration is the cooperation length, which is of the order of a few hundred attoseconds for hard x-ray FELs. The cooperation length scales in good approximation linearly with the radiation wavelength;

therefore, it is more difficult to produce short FEL pulses for soft x-rays than for hard x-rays.

Sub-femtosecond FEL pulses in the hard x-ray regime have been generated by either strong nonlinear compression of a low-charge (≈10–20 pC) electron beam[17,18] or by limiting the lasing of a standard-charge (≈200 pC) electron bunch to a small region using spoiling methods.[19,20] So far, sub-femtosecond pulses in the soft x-ray regime have been produced for standard-charge electron beams with the ESASE mechanism.[21,22] The original idea[21] was to induce an energy modulation in the electron beam in a wiggler with the help of an external laser and later convert the energy modulation to a density modulation in a magnetic chicane. The method has been demonstrated as originally proposed[22] and also by generating the energy modulation in a small longitudinal fraction of the beam without using an external laser.[23]

In this letter, we demonstrate the generation of coherent sub-femtosecond FEL pulses in the soft x-ray regime by fully compressing a low-charge electron beam. We employ nonlinear full compression, as performed previously in Refs. 17 and 18, for the hard x-ray regime. Nonlinear compression, where higher-order transport elements dominate the profile, is preferred to linear compression at

very strong compression factors since it is much more robust against jitters in the radiofrequency (RF) accelerator cavities of the FEL facility.[24] The demonstration has been performed at Athos,[25] the soft x-ray beamline of SwissFEL.[10] The approach has certain advantages with respect to previous work.[21–23] The method does not require any additional hardware besides the standard components of an FEL facility. For SwissFEL, and perhaps also for other facilities, operating with low-charge electron beams has the additional advantage of having fewer issues related to beam loss.

Figure 1 displays a sketch of SwissFEL. Two bunches separated by 28 ns are produced at a repetition rate of 100 Hz and accelerated up to 300 MeV in the injector, which includes five S-band (3 GHz) RF stations and one X-band (12 GHz) RF station. Linac 1 and linac 2, made of C-band (5.7 GHz) RF sections, accelerate the two bunches further up to an energy of 3.17 GeV. Two magnetic chicanes called bunch compressors 1 and 2 (BC1 and BC2) longitudinally compress the bunches after the injector and linac 1, respectively. After linac 2, the second bunch is sent to the switchyard and the Athos beamline with a fast kicker, while the first bunch continues straight for further acceleration in linac 3 and toward the Aramis beamline. The FEL wavelength depends on the electron beam energy and the undulator parameters as[11]

$$\lambda = \frac{\lambda_u}{2\gamma^2}\left(1 + \frac{K^2}{2}\right),\qquad(1)$$

where γ is the Lorentz factor of the electron beam, λ_u is the undulator period, and K is the undulator deflection parameter. The Aramis beamline consists of 13 modules, each of which has a length of 4 m, a period of 15 mm, and a maximum deflection parameter K of 1.8. The Athos beamline consists of 16 units with a length of 2 m each, a period of 38 mm, and a maximum K value of 3.8. Aramis covers a photon energy range between 1.8 and 12.4 keV, while Athos produces FEL radiation with photon energies between 0.26 and 1.9 keV. In both beamlines, the photon energy tuning is achieved by both changing the electron beam energy and the K parameter of the undulator modules. The energy of the Athos bunch can presently be tuned by about ±240 MeV with one C-band RF station.

SwissFEL normally operates with electron beams with a charge of 200 pC. For the results shown here, we operated with bunch charges of 10 pC. The results presented here for Athos were obtained in parallel operation with the Aramis beamline, which was also

working with a fully compressed low-charge beam to deliver sub-femtosecond pulses to scientific users at the Cristallina experimental station.

We generate in the injector an electron beam with a charge of 10 pC and an rms pulse duration of 1.3 ps. We use three dispersive sections to compress the electron beam prior to its injection into the Athos undulator: BC1, BC2, and the switchyard, with longitudinal dispersion R_{56} values of 63.3, 20.6, and 2.2 mm, respectively. Using three compression stages instead of the usual two is helpful to render operations more robust against RF jitters.[18,26] The injector and linac 1 RF phases are chosen in such a way that the beam is fully compressed at the Athos undulators. The RF settings of the second bunch can be tuned independently of the first bunch.[27] Besides tuning the compression settings, we also optimized the number of undulator modules and the reverse taper amplitude for maximum FEL power at the core of the bunch. Reverse taper is necessary to compensate for the large energy chirp in the electron bunch due to space-charge forces.[28,29]

Three main diagnostics are used to characterize and optimize the electron beam and the FEL radiation at Athos. First, we employ an X-band RF transverse deflecting structure (TDS)[30] to measure the longitudinal phase space (LPS) of the electron beam (energy vs time) after the undulator. The TDS is placed after the undulator beamline, so it can be used to reconstruct the FEL power profile by comparing the LPS between lasing-on and lasing-off conditions.[31–33] This method may be affected by resolution and FEL slippage effects. A TDS is very important for setup and diagnostic purposes, but it is not strictly necessary since the standard compression monitors may be sufficient to setup a fully compressed electron beam.[17] Second, we employ a photon gas detector to measure the FEL pulse energy.[34] Third, we use a photon spectrometer to measure the FEL spectra.[35] The beamline grating monochromator is the dispersive element of the spectrometer, while a YAG screen and a 2D CMOS detector image the dispersed spectrum at the exit slit plane. We employ the spectrometer to derive the FEL pulse duration from the weighted average spike width.[17,36]

In the following, we present results obtained in two different shifts. On the first day, we operated with a photon energy of 642 eV and an electron beam energy of 3.35 GeV. In the second shift, we produced FEL radiation with a photon energy of 1111 eV and operated with an electron beam energy of 3.42 GeV. For 642 eV, we operated with a K value of 2.6; we worked with 11 undulator modules (from the fifth to the fifteenth), and we found the optimum taper to be a K increase of 0.0012 per module. For 1111 eV, the K value was
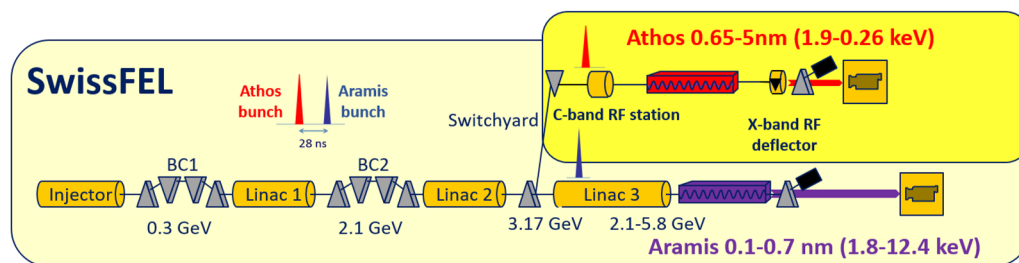
FIG. 1. Schematic layout of SwissFEL and its two beamlines: the hard x-ray beamline Aramis and the soft x-ray beamline Athos.

1.8. We operated with all 16 modules except the last one, with a K increase of 0.0025 per module. The X-band TDS was only available during the first measurement shift.

Figure 2 shows a single-shot image of the final LPS of the electron beam for 642 eV for lasing-enabled and lasing-disabled conditions, as well as the FEL power profile reconstruction obtained by comparing the LPS for the two conditions. The pulse energy for this case was around 20 μJ. The lasing was disabled by slightly detuning the undulator modules. The imprint of the FEL process is clearly visible in the core of the bunch, where the central energy is reduced and the energy spread is increased. The time axis was calibrated by synchronously recording the horizontal centroid of the streaked image and the RF phase for hundreds of shots. The resulting calibration was 45.0 ± 2.1 μm/fs. The energy axis was obtained with the transverse dispersion value of 0.3 m defined by the dipole and quadrupole magnets before the screen. In the figure, one can observe the characteristic K-shape resulting from the space-charge forces of a fully compressed electron beam (as anticipated in simulations and also observed in Ref. 18). The bottom plot of the figure displays the reconstructed FEL power profile for 20 consecutive shots, which is obtained from the time-resolved energy loss of the electrons due to lasing. In the figure, the pulses are aligned in time for better visualiz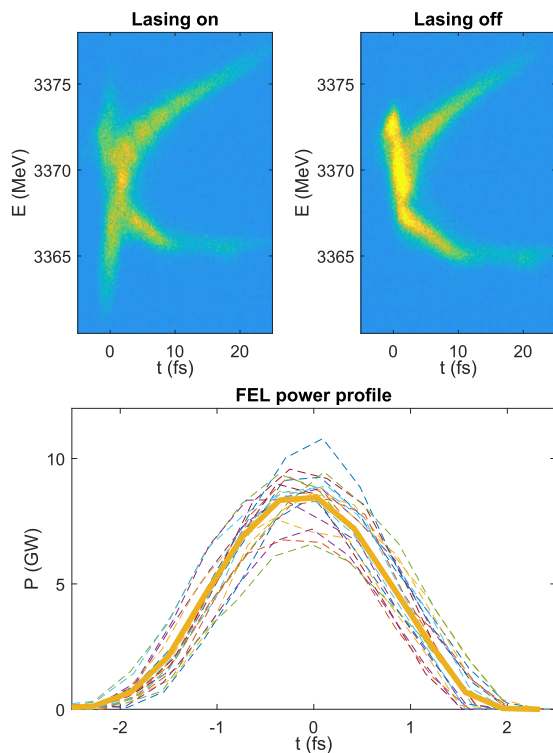ation. As a reference for lasing-off conditions, we take the median of the time-resolved energy over 20 additional shots when lasing was disabled. This reference value is then compared to the time-resolved energy of the lasing-on conditions on a shot-to-shot basis. The time-resolved energies are obtained from the LPS measurements, as shown for a single shot in the top plots of Fig. 2. The dashed lines in the plot correspond to the single shot power profiles, while the solid line indicates the average value over all shots. The total pulse energy obtained using this method, which considers the time-resolved energy loss as well as the electron beam current, fits very well with the pulse energy measured by the gas detector. The reconstructed average FEL rms pulse duration and peak power over the 20 shots are 0.76 ± 0.05 fs and 8.6 ± 1.0 GW. The minimum pulse duration over the 20 shots is 0.69 fs. The reconstructed pulse duration is limited by the present time resolution of the TDS, which was found to be at similar values as the measured pulse duration, and by slippage effects. Therefore, we can expect the true pulse duration to be significantly lower than the reconstructed values and, correspondingly, the peak power to be higher. Moreover, we can expect the pulses to look less uniform than shown in the figure. Nevertheless, to our knowledge, these are the shortest pulse durations ever obtained from time-resolved measurements of the electron beam.

Figure 3 shows the measured spectra for the 642 and 1111 eV cases. The average pulse energies were around 20 and 5 μJ, respectively. In both configurations, more than 70% of the spectra consist of a single spike, and the rest consist of two spikes; therefore, most of the pulses are longitudinally coherent. The FWHM (full width at

FIG. 2. Time-resolved results for a photon energy of 642 eV. Top: single-shot image of the electron beam LPS for lasing-on (left) and lasing-off (right) conditions. Bottom: FEL power profile reconstruction. The dashed lines indicate 20 consecutive shot-to-shot values, while the solid line shows the average value over the 20 shots. See the text for more details.
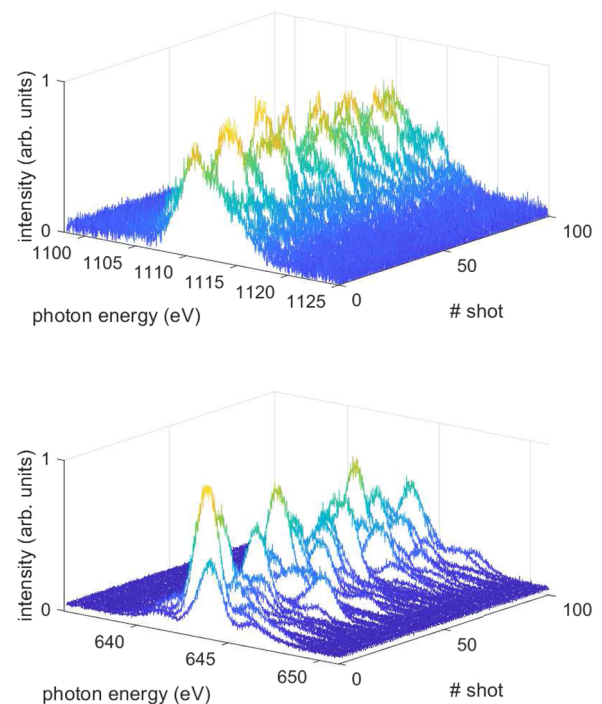

FIG. 3. Spectral results. Top: 100 consecutive single-shot measured spectra for a central photon energy of 1111 eV. Bottom: The same for a central photon energy of 642 eV.

half maximum value) spectral bandwidth averaged over 100 shots is 2.18 ± 0.53 eV for 642 eV and 5.11 ± 1.09 eV for 1111 eV.

We reconstruct the FEL rms pulse duration σ_t from the spike width using the following equation:[17]

$$\sigma_t = \frac{\sqrt{\ln 2}}{\pi\sqrt{\Delta f^2 + \sqrt{\Delta f^4 - (4\ln 2\alpha f_0/\pi)^2}}}, \tag{2}$$

where Δf is the FWHM spectral bandwidth in Hertz, f_0 is the central frequency in Hertz, and α is the photon chirp defined as the relative change of instantaneous frequency over time.

We estimate the photon chirp in two ways. First, we obtain the electron beam chirp from the measured LPS of the electron beam for the 642 eV case (see Fig. 2). We perform a linear fit to the LPS of the lasing-off conditions at the core region of the bunch that lases. This gives an electron beam chirp of about 3 MeV/fs or 8.9×10^{11} s^{-1}. This, considering that the relative FEL chirp is about twice the relative electron beam chirp [see Eq. (1)], translates to $\alpha = 1.78 \times 10^{12}$ s^{-1}. Second, the electron beam chirp can be estimated from the optimum taper amplitude as[23]

$$\frac{d\gamma/\gamma}{dt} = c\frac{K}{2+K^2}\frac{dK}{dz}\frac{\lambda_u}{\lambda}, \tag{3}$$

where c is the speed of light, $\frac{dK}{dz}$ is the optimum taper amplitude, i.e., the optimum variation of the K parameter along the position in the undulator beamline z. The optimum taper amplitude was 4.29×10^{-4} m^{-1} and 8.93×10^{-4} m^{-1} for 642 and 1111 eV, respectively, corresponding to an electron beam chirp of 7.47×10^{11} s^{-1} and 3.12×10^{12} s^{-1}, and to an FEL chirp of $\alpha = 1.49 \times 10^{12}$ s^{-1} and $\alpha = 6.24 \times 10^{12}$ s^{-1}. For the 642 eV photon energy, the chirp estimation from the two methods agrees within 20%.

We can now calculate the photon pulse duration using Eq. (2) (for 642 eV, we take the photon chirp as the average of the two obtained values). The rms pulse duration averaged over all shots is 0.40 ± 0.10 fs for 642 eV and 0.19 ± 0.04 fs for 1111 eV. For 642 eV, these numbers are significantly lower than the values obtained from the LPS in Fig. 2. This is expected since, as mentioned earlier, the LPS values are limited by resolution and slippage effects. An even larger disagreement could be expected for a photon energy of 1111 eV, since here the reconstructed pulse duration from spectral information is shorter than for 642 eV (although slippage effects would be less important at 1111 eV).

To conclude, we have demonstrated the generation of coherent sub-femtosecond FEL pulses in the soft x-ray regime by nonlinear compression. The average FEL rms pulse duration estimated from spectral diagnostics is about 0.4 fs for 642 eV and 0.2 fs for 1111 eV. Time-resolved diagnostics of the electron beam, somewhat limited by resolution and slippage effects, indicate FEL pulse durations of about 0.75 fs or less for 642 eV. The method is simple, does not require any additional hardware, and can be implemented at any existing or planned FEL facility. It employs a low-charge electron beam, which in principle corresponds to fewer issues related to beam loss. We think that our work will open the door for significant advances in ultrafast FEL applications in the soft x-ray

regime, making sub-femtosecond pulses widely available for user experiments.

AUTHOR DECLARATIONS

Conflict of Interest

The authors have no conflicts to disclose.

Author Contributions

Eduard Prat: Conceptualization (lead); Data curation (lead); Formal analysis (equal); Funding acquisition (equal); Investigation (lead); Methodology (equal); Project administration (lead); Resources (equal); Software (equal); Supervision (equal); Validation (equal); Visualization (lead); Writing – original draft (lead); Writing – review & editing (equal). **Alexander Malyzhenkov**: Conceptualization (lead); Data curation (supporting); Formal analysis (equal); Funding acquisition (equal); Investigation (lead); Methodology (equal); Project administration (supporting); Resources (equal); Software (equal); Supervision (equal); Validation (equal); Visualization (supporting); Writing – original draft (supporting); Writing – review & editing (equal). **Christopher Arrell**: Conceptualization (supporting); Data curation (supporting); Formal analysis (equal); Funding acquisition (equal); Investigation (supporting); Methodology (equal); Project administration (supporting); Resources (equal); Software (equal); Supervision (equal); Validation (equal); Visualization (supporting); Writing – original draft (supporting); Writing – review & editing (equal). **Paolo Craievich**: Conceptualization (supporting); Data curation (supporting); Formal analysis (equal); Funding acquisition (equal); Investigation (supporting); Methodology (equal); Project administration (supporting); Resources (equal); Software (equal); Supervision (equal); Validation (equal); Visualization (supporting); Writing – original draft (supporting); Writing – review & editing (equal). **Sven Reiche**: Conceptualization (lead); Data curation (supporting); Formal analysis (equal); Funding acquisition (equal); Investigation (supporting); Methodology (equal); Project administration (lead); Resources (equal); Software (equal); Supervision (equal); Validation (equal); Visualization (supporting); Writing – original draft (supporting); Writing – review & editing (equal). **Thomas Schietinger**: Conceptualization (supporting); Data curation (supporting); Formal analysis (equal); Funding acquisition (equal); Investigation (supporting); Methodology (equal); Project administration (lead); Resources (equal); Software (equal); Supervision (equal); Validation (equal); Visualization (supporting); Writing – original draft (supporting); Writing – review & editing (equal). **Guanglei Wang**: Conceptualization (supporting); Data curation (supporting); Formal analysis (equal); Funding acquisition (equal); Investigation (supporting); Methodology (equal); Project administration (supporting); Resources (equal); Software (equal);

Supervision (equal); Validation (equal); Visualization (supporting); Writing – original draft (supporting); Writing – review & editing (equal).

DATA AVAILABILITY

The data that support the findings of this study are available from the corresponding author upon reasonable request.

REFERENCES

[1] Z. Huang and K.-J. Kim, Phys. Rev. Spec. Top.-Accel. Beams **10**, 034801 (2007).

[2] B. W. J. McNeil and N. R. Thompson, Nat. Photonics **4**, 814 (2010).

[3] C. Pellegrini, A. Marinelli, and S. Reiche, Rev. Mod. Phys. **88**, 015006 (2016).

[4] W. Ackermann, G. Asova, V. Ayvazyan, A. Azima, N. Baboi, J. Bähr, V. Balandin, B. Beutner, A. Brandt, A. Bolzmann et al., Nat. Photonics **1**, 336 (2007).

[5] P. Emma, R. Akre, J. Arthur, R. Bionta, C. Bostedt, J. Bozek, A. Brachmann, P. Bucksbaum, R. Coffee, F.-J. Decker et al., Nat. Photonics **4**, 641 (2010).

[6] T. Ishikawa, H. Aoyagi, T. Asaka, Y. Asano, N. Azumi, T. Bizen, H. Ego, K. Fukami, T. Fukui, Y. Furukawa et al., Nat. Photonics **6**, 540 (2012).

[7] E. Allaria, D. Castronovo, P. Cinquegrana, P. Craievich, M. Dal Forno, M. B. Danailov, G. D'Auria, A. Demidovich, G. De Ninno, S. Di Mitri et al., Nat. Photonics **7**, 913 (2013).

[8] H.-S. Kang, C.-K. Min, H. Heo, C. Kim, H. Yang, G. Kim, I. Nam, S. Y. Baek, H.-J. Choi, G. Mun et al., Nat. Photonics **11**, 708 (2017).

[9] W. Decking, S. Abeghyan, P. Abramian, A. Abramsky, A. Aguirre, C. Albrecht, P. Alou, M. Altarelli, P. Altmann, K. Amyan et al., Nat. Photonics **14**, 391 (2020).

[10] E. Prat, R. Abela, M. Aiba, A. Alarcon, J. Alex, Y. Arbelo, C. Arrell, V. Arsov, C. Bacellar, C. Beard et al., Nat. Photonics **14**, 748 (2020).

[11] R. Bonifacio, C. Pellegrini, and L. M. Narducci, Opt. Commun. **50**, 373 (1984).

[12] J. Amann, W. Berg, V. Blank, F.-J. Decker, Y. Ding, P. Emma, Y. Feng, J. Frisch, D. Fritz, J. Hastings et al., Nat. Photonics **6**, 693 (2012).

[13] D. Ratner, R. Abela, J. Amann, C. Behrens, D. Bohler, G. Bouchard, C. Bostedt, M. Boyes, K. Chow, D. Cocco et al., Phys. Rev. Lett. **114**, 054801 (2015).

[14] P. Rebernik Ribič, A. Abrami, L. Badano, M. Bossi, H.-H. Braun, N. Bruchon, F. Capotondi, D. Castronovo, M. Cautero, P. Cinquegrana et al., Nat. Photonics **13**, 555 (2019).

[15] L. Young, K. Ueda, M. Gühr, P. H. Bucksbaum, M. Simon, S. Mukamel, N. Rohringer, K. C. Prince, C. Masciovecchio, M. Meyer et al., J. Phys. B: At., Mol. Opt. Phys. **51**, 032003 (2018).

[16] S. Li, T. Driver, P. Rosenberger, E. G. Champenois, J. Duris, A. Al-Haddad, V. Averbukh, J. C. T. Barnard, N. Berrah, C. Bostedt et al., Science **375**, 285 (2022).

[17] S. Huang et al., Phys. Rev. Lett. **119**, 154801 (2017).

[18] A. Malyzhenkov, Y. P. Arbelo, P. Craievich, P. Dijkstal, E. Ferrari, S. Reiche, T. Schietinger, P. Juranić, and E. Prat, Phys. Rev. Res. **2**, 042018(R) (2020).

[19] A. Marinelli, J. P. MacArthur, P. Emma, M. W. Guetg, C. Field, D. Kharakh, A. A. Lutman, Y. Ding, and Z. Huang, Appl. Phys. Lett. **111**, 151101 (2017).

[20] P. Dijkstal, Ph.D. thesis, ETH Zurich, 2022.

[21] A. A. Zholents, Phys. Rev. Spec. Top.-Accel. Beams **8**, 040701 (2005).

[22] J. P. Duris, J. P. MacArthur, J. M. Glownia, S. Li, S. Vetter, A. Miahnahri, R. Coffee, P. Hering, A. Fry, M. E. Welch et al., Phys. Rev. Lett. **126**, 104802 (2021).

[23] J. Duris, S. Li, T. Driver, E. G. Champenois, J. P. MacArthur, A. A. Lutman, Z. Zhang, P. Rosenberger, J. W. Aldrich, R. Coffee et al., Nat. Photonics **14**, 30 (2019).

[24] S. Huang, Y. Ding, Z. Huang, and J. Qiang, Phys. Rev. Spec. Top.-Accel. Beams **17**, 120703 (2014).

[25] E. Prat, A. Al Haddad, C. Arrell, S. Augustin, M. Boll, C. Bostedt, M. Calvi, A. L. Cavalieri, P. Craievich, A. Dax et al., Nat. Commun. **14**, 5069 (2023).

[26] H.-S. Kang, H. Yang, G. Kim, H. Heo, I. Nam, C.-K. Min, C. Kim, S. Y. Baek, H.-J. Choi, G. Mun et al., J. Synchrotron Radiat. **26**, 1127 (2019).

[27] M. Paraliev, A. Alarcon, V. Arsov, S. Bettoni, R. Biffiger, M. Boll, H. Braun, A. Citterio, P. Craievich, A. Dax et al., Phys. Rev. Accel. Beams **25**, 120701 (2022).

[28] E. L. Saldin, E. A. Schneidmiller, and M. V. Yurkov, Phys. Rev. Spec. Top.-Accel. Beams **9**, 050702 (2006).

[29] Y. Ding, Z. Huang, D. Ratner, P. Bucksbaum, and H. Merdji, Phys. Rev. Spec. Top.-Accel. Beams **12**, 060703 (2009).

[30] P. Craievich, M. Bopp, H.-H. Braun, A. Citterio, R. Fortunati, R. Ganter, T. Kleeb, F. Marcellini, M. Pedrozzi, E. Prat et al., Phys. Rev. Accel. Beams **23**, 112001 (2020).

[31] Y. Ding, C. Behrens, P. Emma, J. Frisch, Z. Huang, H. Loos, P. Krejcik, and M.-H. Wang, Phys. Rev. Spec. Top.-Accel. Beams **14**, 120701 (2011).

[32] C. Behrens, F.-J. Decker, Y. Ding, V. A. Dolgashev, J. Frisch, Z. Huang, P. Krejcik, H. Loos, A. Lutman, T. J. Maxwell et al., Nat. Commun. **5**, 3762 (2014).

[33] P. Dijkstal, A. Malyzhenkov, P. Craievich, E. Ferrari, R. Ganter, S. Reiche, T. Schietinger, P. Juranić, and E. Prat, Phys. Rev. Res. **4**, 013017 (2022).

[34] A. A. Sorokin, Y. Bican, S. Bonfigt, M. Brachmanski, M. Braune, U. F. Jastrow, A. Gottwald, H. Kaser, M. Richter, and K. Tiedtke, J. Synchrotron Radiat. **26**, 1092 (2019).

[35] C. Arrell, V. Thominet, Y. Arbelo, U. Wagner, N. Gradwohl, E. Prat, L. Patthey, and R. Follath, in Conference on Lasers and Electro-Optics (Optica Publishing Group, 2022).

[36] Y. Inubushi, K. Tono, T. Togashi, T. Sato, T. Hatsui, T. Kameshima, K. Togawa, T. Hara, T. Tanaka, H. Tanaka et al., Phys. Rev. Lett. **109**, 144801 (2012).